

A HPGR pseudo-dynamic model approach integrated with real-time information for pressing iron ore concentrates in industrial-scale

T M Campos¹, H A Petit², R Olympio³ and L M Tavares⁴

1. Research assistant, Department of Metallurgical and Materials Engineering, Universidade Federal do Rio de Janeiro, 21941–972. Email: tulio.campos@coppe.ufrj.br
2. Post-doctoral fellow, D.Sc, Department of Metallurgical and Materials Engineering, Universidade Federal do Rio de Janeiro, 21941–972. Email: hpetit@metalmat.ufrj.br
3. Engineer, M.Sc, Vale S.A, Complexo de Tubarão, 29090–860. Email: ricardo.olympio@vale.com
4. Professor, Ph.D., Department of Metallurgical and Materials Engineering, Universidade Federal do Rio de Janeiro, 21941–972. Email: tavares@metalmat.ufrj.br

ABSTRACT

Much practical experience has been gathered in the last 30 years of application of high-pressure grinding rolls (HPGR) integrated with ball milling in size reduction of fine iron ore concentrates. The company Vale S.A, in Complexo de Tubarão (Brazil), was one of the pioneers applying the technology prior to pelletisation with an outstanding size reduction energy efficiency in the circuit and a significant increment in the specific surface area of the product. Recent studies by the authors demonstrated benefits of modelling and simulation to improve the performance of HPGRs in this particular application, with the model being able to describe HPGR performance under different operating conditions and under variations of feed size distribution. Despite these important advances, this modelling approach has only been used offline and under steady-state conditions. The present work applies the modified Torres and Casali model proposed by the authors in pseudo-dynamic simulations. The ability of the model to predict the characteristics of the product in real-time is evaluated using data available online for the pellet feed preparation circuit. Results demonstrated the model capabilities to map the physical operation and give a realistic representation of the process. Additionally, the model is demonstrated to be able to support the pellet feed production by providing extended real-time information of the process, making it a useful tool for improvement of the operational strategies and process stability.

INTRODUCTION

High-pressure grinding rolls (HPGR) reached great popularity in the last 30 years of application in the minerals industry. The company Vale S.A, in the Complexo de Tubarão (Vitória, Brazil), was one of the pioneers using this technology for pressing iron ore concentrates in integrated circuits with ball milling (Van der Meer, 1997), where the HPGR usually operates in the regrinding prior to pellet formation in the so-called pellet feed preparation stage. The success of HPGRs in this type of application can be summarised by their capabilities to improve the Blaine specific surface area (BSA) coupled with a high throughput and low specific energy consumption (Van der Meer, 2010; Abazarpour *et al*, 2018; Campos *et al*, 2019a). In this particular circuit configuration, the HPGR represents the interface between the end of the pellet feed preparation circuit and the beginning of the pellet formation process (Campos *et al*, 2019a), so that the technology occupies a key position in potentially absorbing disturbances caused in upstream operations and producing a qualified iron ore pellet feed to the downstream process.

Aiming to support operations, advances in the mathematical modelling describing HPGR performance followed, at least in parts, the improvement in the technology over the last 40 years (Rashidi *et al*, 2017). Among several works considering simplest and empirical modelling approaches (Chelgani *et al*, 2021), going through phenomenological models (Morrell *et al*, 1997; Torres and Casali, 2009; Dundar *et al*, 2013) and more in-depth descriptions with simulations using the discrete element method (Barrios and Tavares, 2016; Cleary and Sinnott, 2021; Rodriguez *et al*, 2021, 2022), improvements have been made possible in operations. New dynamic modelling approaches have been proposed, showing potential to be used as model predictive control in industrial-scale HPGRs (Numbi and Xia, 2015; Johansson and Evertsson, 2019; Vyhmeister *et al*, 2019) and to help improve understanding towards process integration. Nevertheless, the simplicity

of some of the descriptions and the very limited level of validation of some of these approaches raise several questions regarding their applicability. In the particular case of interest in the present work regarding pressing iron ore concentrates, published works by the authors (Campos *et al*, 2019b, 2021) proposed and demonstrated the validity of several modifications to the phenomenological HPGR model proposed by Torres and Casali (2009), applying it to both pilot – and industrial-scale HPGRs operating under a range of conditions. However, applications were limited to offline simulations and to steady state conditions.

Indeed, the new digital transformation in the minerals industry is shifting traditional operation towards new approaches that are able to correlate dynamic modelling with industrial demands from real-time simulations. Robust models providing rapid and accurate responses coupled with an integration into the plant network and real-time information between the physical operation and the digital models will, potentially, allow predicting variations within the process besides being the basis of a robust model-predictive control. Despite these potential improvements, several key challenges still remain when it comes to HPGR full process integration and multi-scale dynamic modelling within pellet feed preparation circuits for long periods.

The present work proposes a new modelling approach integrated with real-time information and uses it in pseudo-dynamic simulations of size reduction of iron ore concentrates in an industrial-scale HPGR. Model prediction is investigated in a period of a year of operation and applied to describe HPGR performance under different roll surface wear conditions. A new method is proposed and applied to improve model prediction when dealing with worn rolls.

MODELLING BACKGROUND

Among the main phenomenological mathematical models that are able to describe the HPGR performance (Morrell *et al*, 1997; Torres and Casali, 2009; Dundar *et al*, 2013), the approach proposed by Torres and Casali (2009) is able to predict power consumption and throughput on the basis of physical equations on the operations, besides describing the size reduction based on the population balance model. Recent works by the authors identified some limitations on the model when dealing with Brazilian iron ores and proposed some particular modifications to model equations with the aim of improving prediction (Campos *et al*, 2019b, 2021).

Briefly, the so-called modified Torres and Casali model (Campos *et al*, 2019b, 2021) relies on the plug flow model to calculate the HPGR throughput as:

$$Q = U_g L \chi_g \rho_g \left(\frac{100}{100 - \delta} \right) \quad (1)$$

where U_g is the material velocity, χ_g is the operating gap, L is the roll length, ρ_g is the flake density and δ is a parameter representing the proportion of material ejected by the edge of the rolls given by:

$$\ln \left(\frac{\delta}{\varphi} \right) = -v \frac{\chi_g}{D} \left(\frac{U}{U_{max}} \right)^\tau \quad (2)$$

where D is the roll diameter, U is the roll velocity, U_{max} is the maximum roll velocity allowed for the machine and φ , v and τ are fitting parameters. The material velocity in Equation 1 is estimated as:

$$U_g = \frac{U \rho_a \chi_c}{\rho_g \chi_g} \quad (3)$$

where ρ_a is the bulk density and χ_c is the critical size given by $\chi_c = \chi_g + D(1 - \cos \alpha_{ip})$.

The power consumption prediction is carried out based on the torque for both rollers multiplied by the angular roll velocity as:

$$P = 2F_m \sin \left(\frac{\kappa \alpha_{ip}}{2} \right) U \quad (4)$$

where α_{ip} is the nip angle, κ is a fitting parameter that allows adjusting the estimate of the nip angle and F_m is the compressive force applied to the particle bed (Torres and Casali, 2009):

$$F_m = p_m \frac{D}{2} L \quad (5)$$

where p_m is the hydraulic pressure.

Finally, the size reduction can be predicted from an analytical solution of the population balance model which allows to calculate the product size distribution ($w_{i,k}$) for N_b section along the axial roll position (Torres and Casali, 2009):

$$w_{i,k} = \sum_{j=1}^i A_{ij,k} \exp\left(-\frac{S_{j,k}}{U_g} z^*\right) \quad (6)$$

where z^* is the distance between the beginning of the compression region and the extrusion zone (Torres and Casali, 2009) and $S_{j,k}$ is the breakage rate for each size class j and section k . The analytical solution uses the non-normalisable breakage function (King, 2001) and the specific selection function approach (Herbst and Fuerstenau, 1980) to solve the differential equations. The cumulative non-normalisable breakage function is given by:

$$B_{ij} = \phi \left(\frac{x_i}{x_j}\right)^\gamma + (1 - \phi) \left(\frac{x_i}{x_j}\right)^\beta \quad \text{for } x_i \geq \omega$$

$$B_{ij} = \phi \left(\frac{x_i}{\omega}\right)^\eta \left(\frac{x_i}{x_j}\right)^\gamma + (1 - \phi) \left(\frac{x_i}{x_j}\right)^\beta \quad \text{for } x_i < \omega$$
(7)

where x_i is the particle size, γ , β , ϕ , ω and η are fitting parameters and b_{ij} is the distributed breakage function calculated from $b_{ij} = B_{i-1,j} - B_{ij}$. The breakage rate, on the other hand, is given by:

$$S_{i,k} = s_i^E \frac{P_k}{H_k} \Psi\left(\frac{P}{Q}\right) \quad (8)$$

where H_k is a constant Hold-up along the roll length, P_k is the power profile and s_i^E is the specific selection function:

$$\ln(s_i^E / s_1^E) = \xi_1 \ln(\hat{x}_i / \hat{x}_1) + \xi_2 [\ln(\hat{x}_i / \hat{x}_1)]^2 \quad (9)$$

where s_1^E , ξ_1 and ξ_2 are fitting parameters, \hat{x}_i is the representative size calculated from $\hat{x}_i = \sqrt{x_i x_{i-1}}$ and \hat{x}_1 is a reference size given by the top size class.

The power profile in Equation 8 allows the model to predict the variation of the product size distribution along the roll length, which is a key feature in HPGR operations. The power profile is then given as:

$$P_k = 2F_m \sin\left(\frac{\kappa \alpha_{ip}}{2}\right) U \frac{P'_k}{\sum_{j=1}^{N_B} P'_j} \quad (10)$$

where P'_k is calculated on the basis of the Fourier Transform and allows the model to describe shape profiles that vary from trapezoidal to a parabolic (Campos *et al*, 2021):

$$P'_k = \frac{4}{\pi} \sum_{n=1}^{100} \frac{1 - \cos n\pi}{2n} e^{-\mu(n^2\pi^2)} \sin n\pi \bar{y}_k \quad (11)$$

where μ is a fitting parameter.

In order to account for the drop of energy efficiency when the specific energies are raised in HPGR operation, a damping parameter multiplying the breakage rate in Equation 8 was proposed (Campos *et al*, 2021):

$$\Psi(E_i) = \exp\left[-\left(\frac{E_i}{E'}\right)^\Lambda\right] \quad (12)$$

where E_i is the specific input energy, E' is a parameter, called energy densification, and λ is a second fitting parameter.

MATERIALS AND METHODS

HPGR operation

An industrial-scale HPGR from one of the pelletising plants from Complexo de Tubarão from Vale S.A (Vitória, Brazil) was selected as case study in the present work. The HPGR operates in an integrated circuit with ball milling and is at the boundary between the end of the pellet feed preparation stage and the beginning of the pellet formation process (Campos *et al*, 2021). The machine was connected to a process information management system (PIMS) in order to capture information on throughput, power consumption, operating pressure, roll peripheral velocity and operating gap. Operating gap was measured using a gap sensor positioned on both edges of the rolls.

Operation is often carried out with a feed moisture content of 8 ± 0.5 per cent, which is closer to the maximum that is tolerated for pressing iron ore concentrates (Van der Meer, 1997). Table 1 summarises the main HPGR settings and range allowed for the operating conditions. Given the large roll dimensions, this HPGR faces a particular issue operating below the designed capacity since the feed hopper does not allow to keep the HPGR operating in a choke fed condition and, therefore, drives the machine to operate under roll peripheral velocities lower than the original value allowed (Table 1).

TABLE 1
Summary of the main HPGR settings and operating ranges.

Variable	Value
Roll diameter (m)	2.25
Roll length (m)	1.55
Specific force (N/mm ²)	0.5–5.5
Operating pressure (bar)	20–180
Roll velocity (m/s)	0.2–2.01
Operating gap (mm)*	5–15
Nominal throughput (t/h)	400–1200
Total power consumption (kW)	500–3600

As previous investigated by the authors (Campos *et al*, 2021), the HPGR is fed with a blend of four different iron ore concentrates mainly composed of hematite with minor amounts of quartz as contaminant. Specific gravity of the feed was measured by Helium Pycnometry, being equal to 4.9 t/m^3 . The bulk density was determined from the ratio between the sample mass in a known volume after vibration and given as 3.0 t/m^3 , whereas the flake density was measured using preserved flakes from Archimedes principle and given as 3.54 t/m^3 .

In order to ensure a careful investigation about HPGR operation when machine is under different roll wear patterns, measurements of the distance between the top of the studs and a metal strip placed in the front of the rolls along the axial position were carried out as presented in Figure 1. This distance between the roll surface and the metal strip was measured periodically in 63 studs selected in both rollers using a digital calliper. It is worth mentioning that the authors recognise that recent works presented more reliable and accurate approaches to measure the wear pattern from online systems (Burchardt and Mackert, 2019), but the approach adopted in the present work was also used and already validated elsewhere (Rodriguez *et al*, 2021).

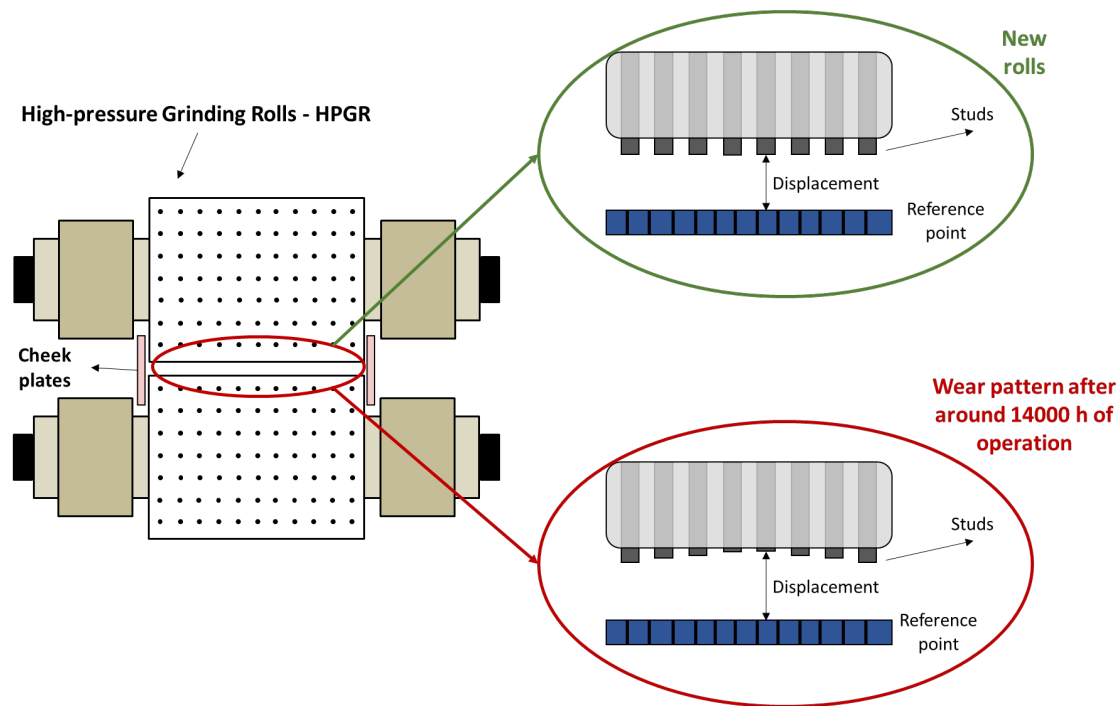


FIG 1 – Schematic diagram showing the experimental device used to measure the distance between a reference position and the top of 63 studs along the roll length. The green circle presents the rolls in the beginning of the wear life, whereas the red circle presents an illustration of the worn profile after 14 000 hours of operation, which is usually the total wear lifetime.

Data collection

A period of 12 months was selected with information recorded in a frequency of 5 min from PIMS, which corresponds to around 105 120 data points for a total of five variables in HPGR operation. Assuming no information about HPGR feed and product in real-time, samples were gathered from the process every four hours in the entire period evaluated. A sampler was used to collect material, whereas BSA was measured in laboratory using a PCBlaine-Star (Zünderwerke Ernst Brün GmbH). A total of 2190 points were recorded in this second data set.

To ensure that the data collected from the process was reliable, two steps were used in the present work. First, considering the lack of uniformity in the sampling rates between the PIMS data set and the laboratory data set, a regularisation between both was necessary. For this purpose, the BSA measurement was assumed as an average of the last four hours within the process and, therefore, its value repeated for these previous four hours considering the frequency of 5 min adopted in the PIMS data set. Considering the new regularised data, the second step relied on cleaning the data to avoid missing values, outliers, measurement disturbances and low accuracy in all process variables. Data deletion strategy was adopted to overcome missing values, which is a valid approach when the amount of missing data is only a negligible fraction of the entire data set. In order to remove outliers, a preliminary operation consisted of removing data when they do not satisfy physical conditions and usual operating ranges presented in Table 1. Outliers were also identified and removed when a value for a data point was more than three scaled median absolute relative deviations from the median (MAD). After data reconciliation and data cleaning a set of 65 193 data points for each HPGR variable was then used for modelling and simulation.

Model implementation

The modified Torres and Casali model (Campos *et al*, 2019b, 2021) was implemented in Matlab™ (version R2021b, Mathworks Inc) to perform all the simulations. A nonlinear optimisation method was used to calibrate the breakage parameters (Table 1), which basically relies in a function available in Matlab, called *fminsearch*, able to find the minimum of a multivariable scalar function using the Nelder-Mead method from an initial estimation. The objective function consisted of the sum of the differences of the logarithms of the experimental and the fitted values of the particle size distribution of a reference test (Base Case) in cumulative form using the least squares method:

$$f_{obj} = \sum_{i=1}^N \left[\log \left(W_{Calc}^{HPGR}(i) \right) - \log \left(W_{Exp}^{HPGR}(i) \right) \right]^2 \quad (13)$$

where N is the number of size classes, W_{Calc}^{HPGR} and W_{Exp}^{HPGR} are, respectively, the calculated and experimental fraction passing in size i . The objective function was proposed in the logarithmic form in order to ensure a more reliable description of the fine part of the size distribution, since the present work aims to quantify this part of the distribution accurately.

The online model structure relied on the application of the Modified Torres and Casali model coupled with real-time information about HPGR operating conditions and feed characteristics. Predictions are evaluated on the basis of the absolute relative deviation from measurements and from time series comparisons.

RESULTS

Process results

Data collected from PIMS and filtered following each step presented in the Section ‘HPGR operation’ was analysed in the entire period. Statistical analysis provided detailed information about operating conditions and HPGR performance variables, which were analysed in light of global variation in the entire period and local variations when dealing with each specific month.

Rolls wear patterns were carefully investigated in the entire period. Figure 2 shows wear profiles in the beginning, middle and end of rolls lifetime. A trapezoidal (also named ‘bathtub’) profile already discussed and investigated elsewhere (Gardula *et al*, 2015; Burchardt and Mackert, 2019; Rodriguez *et al*, 2021), is evident in the beginning, whereas a parabolic profile is reached when the HPGR is closer to 14 000 hours of operation, which is typically the maximum lifetime for the rolls in operation. Wear profiles were concave and more intensive wear occurred in the middle of the rolls, besides presenting modest wear on the edge region up to the middle lifetime and a significant edge effect when the parabolic wear profile was achieved in the end of its lifetime. Results are lined up with previous investigations carried out using DEM (Rodriguez *et al*, 2021) and from industrial-scale measurements for pressing iron ores (Nejad and Sam, 2017).

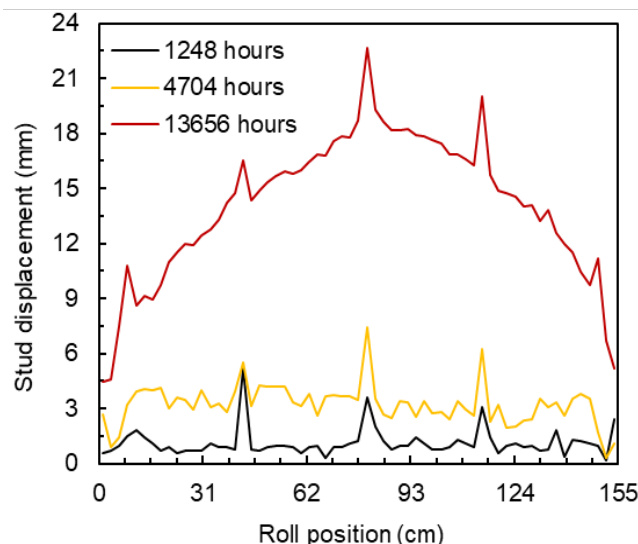


FIG 2 – Roll wear patterns registered from the beginning of operation up to the end of roll wear lifetime with nearly 14 000 hours of operation.

Figure 3 presents the average variation of operating pressure (a) and roll peripheral velocity (b) in the twelve months investigated, whereas vertical lines represent the standard deviation for each month. Figure 3a shows the minor global variation of the roll peripheral velocity, in which average values varied from 1.00 to 1.04 m/s. The very small standard deviation for each month (up to 0.04 m/s) also confirms that this process variable varies within a very narrow range of operating conditions. As discussed in Section ‘HPGR operation’, the HPGR investigated does not allow to

ensure a choke fed condition when dealing with high throughputs (higher than 650 t/h), thus imposing nearly constant roll velocities throughout its operation. Additionally, Figure 3a allows to conclude a potential improvement study in the HPGR performance since the roll velocity is a well-known controlled variable used to change throughput and power consumption of HPGRs (Johansson and Evertsson, 2019; Vyhmeister *et al*, 2019). Operating pressure, which is the key variable used to improve size reduction, presented monthly averages from 56.7 to 66.9 bar and standard deviations for each month up to 7.1 bar (Figure 3b). Local variation in the operating pressure in each month can be related to the control strategy adopted in order to maintain constant the torque in both rollers, besides potentially absorbing variations in the feed size distribution. A slight, but still important, global variation can be identified after the fifth month. Assuming the drop in size reduction caused by the worn rolls (Figure 2), the increase in operating pressure can be explained, at least in part, as an operational strategy used to overcome this issue.

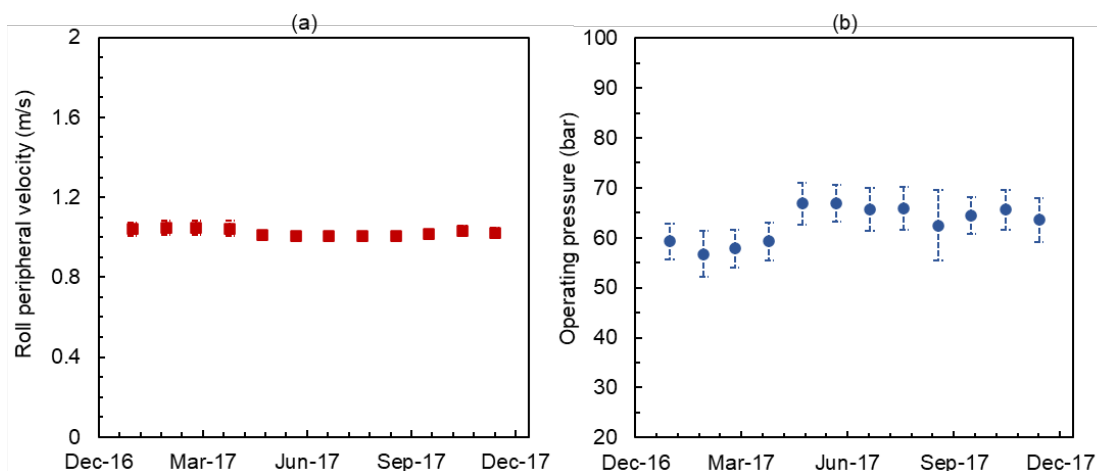


FIG 3 – Month-to-month variation of operating pressure (a) and roll peripheral velocity (b) over a period of 12 months. Markers are the average values for each month and vertical lines present the standard deviations within each month.

Variation of the average value of the measured operating gap in each month is presented in Figure 4. Results showed significant changes in the entire period with average values ranging from 13.0 to 5.1 mm. Unlike the well-known trend between operating pressure and operating gap (Daniel, 2002; Barrios and Tavares, 2016), the minor increase of pressure in Figure 3b does not have a clear relationship with the significant reduction in operating gap. In association to Figures 2 and 3b, the reduction of the operating gap and the poor relationship with operating pressure can be again explained on the basis of roll wear (Figure 2). Indeed, taking into account the approach used to determine the operating gap (Section ‘HPGR operation’) and the usual concave profile of the rolls (Figure 2), it is worth mentioning that measurements of operating gap are only associated to the distance between rollers in the edge, thus not accounting for the parabolic (or bathtub) profile in the centre region. Results from Figure 4 allow to state that operating gap is not a reliable variable in the process when dealing with worn rollers, although it remains valid as an indicator of roll condition.

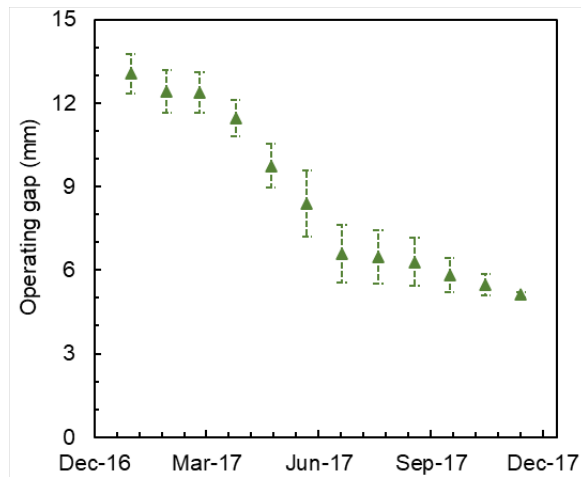


FIG 4 – Month-to-month variation of operating gap over a period of 12 months. Green triangles represent the average values and vertical lines present the standard deviations within each month.

Month-to-month variation of throughput and power consumption in the period investigated are shown in Figure 5. Minor global variations can be seen in the throughput with average values from 531 to 623 t/h. Standard deviation values for each month (vertical lines) reaching 52 t/h also demonstrate that the HPGR throughput varying within a narrow range of operating conditions. Results from Figure 5a are mainly governed by the roll peripheral velocity (Figure 3a), thus explaining its small changes.

On the other hand, Figure 5b presents both average values (from 1523 to 1483 kW) and standard deviations (up to 175 kW) for HPGR power with important variations. Comparing results from Figure 5b and Figure 3b it is possible to argue that power consumption for this HPGR is mainly determined by changes in operating pressure.

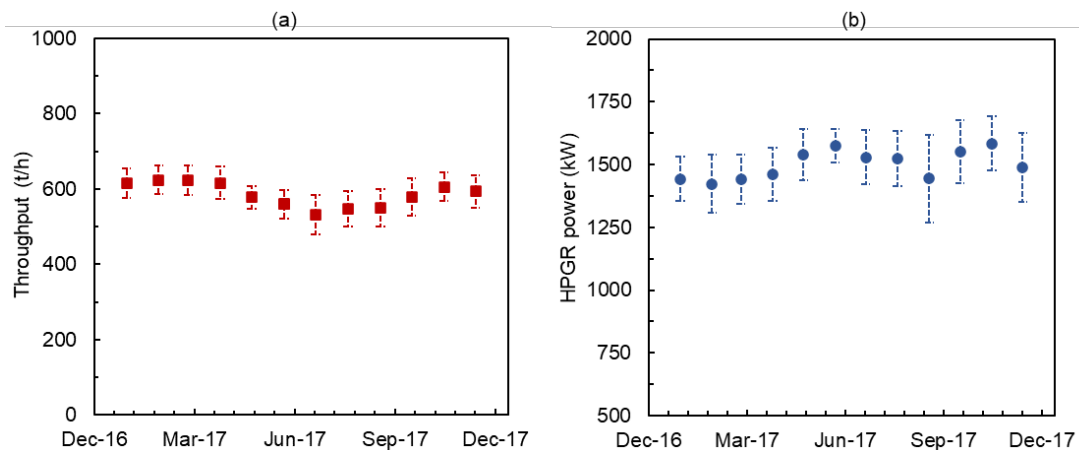


FIG 5 – Month-to-month variation of throughput (a) and power consumption (b) over a period of 12 months. Markers represent the average value, whereas vertical lines are the standard deviations within each month.

Data from laboratory analyses characterising the HPGR feed and product are presented in Figure 6. Important month-to-month variations are evident, with the average value for each month varying from 1550 to 1650 cm²/g in the HPGR feed and from 1770 to 1910 cm²/g in the HPGR product. Important variations within each month, evident from the high standard deviations, also demonstrate the significant changes in both feed and product size. Moreover, results from Figure 6 show that the product BSA is highly influenced by the feed BSA and, beyond the improvement in the product surface area, it is almost ever following the trend imposed by the feed.

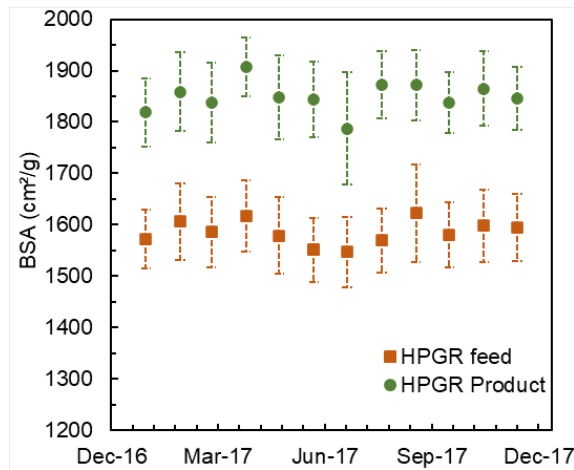


FIG 6 – Month-to-month variation of Blaine specific surface areas of the feed and product of the HPGR over a period of 12 months. Markers represent the average value, whereas vertical lines are the standard deviations within each month.

Power consumption and throughput predictions

Results from Figure 7 compare model predictions and experiments in the entire period assessed for power consumption (a) and throughput (b). Good agreement was reached for the first four months (close to 3000 hours of operation) with average absolute relative deviation from measurements up to 5.8 per cent for the throughput and 6.3 per cent for the power consumption. This period corresponds to the same period when the HGPR was operating from the beginning of lifetime until a point when the roll wear pattern reached a bathtub profile (Figure 2). Although already exhibiting a bathtub wear profile, results from Figure 7 demonstrate the ability of the model in providing good predictions of power and throughput. Under these conditions, the nip angle parameter (κ in Equation 4) was fixed in 2.75. On the other hand, in the case of the throughput model (Equation 2), two parameters were maintained equal to those previous calibration by the authors and given by $\varphi = 100$ and $\tau = 0.1$ (Campos *et al*, 2021), whereas the remaining parameter was fitted ($\nu = 550$).

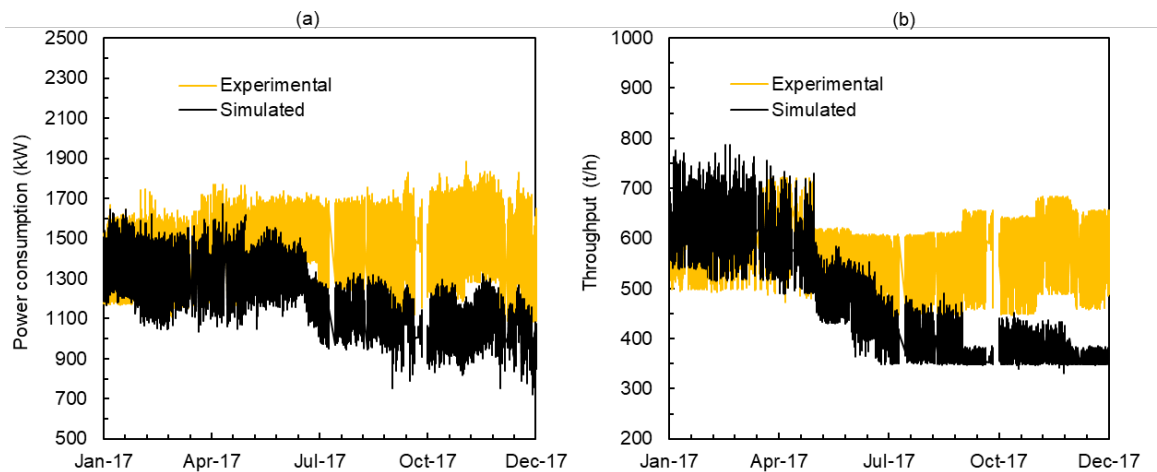


FIG 7 – Comparison of experimental and predicted values for power consumption (a) and throughput (b) in the twelve months investigated. Data is presented for every 5 min of operation.

With the aim of improving the model prediction when dealing with different roll wear patterns (briefly discussed in the Introduction), the present work proposes an algorithm to recalibrate selected parameters of the Modified Torres and Casali model. The step-by-step approach used to recalibrate the model is illustrated in Figure 8, which shows that it consists in a progressive analysis used to verify power consumption and throughput predictions, respectively. A value of absolute relative deviation from measurements of 10 per cent for both power and throughput is used as threshold for model accuracy. If the absolute relative deviation from measurements is higher than 10 per cent for more than one hour of operation, the approach allows the model to recalibrate selected model

parameters, as discussed previously. Parameter optimisation is performed from the difference between calculated and experimental values for a reference test selected in the previous hour of operation using the least square method. Parameter κ in Equation 4 was selected to be recalibrated in the power consumption model, whereas parameter ν was selected for the throughput model (Equation 2).

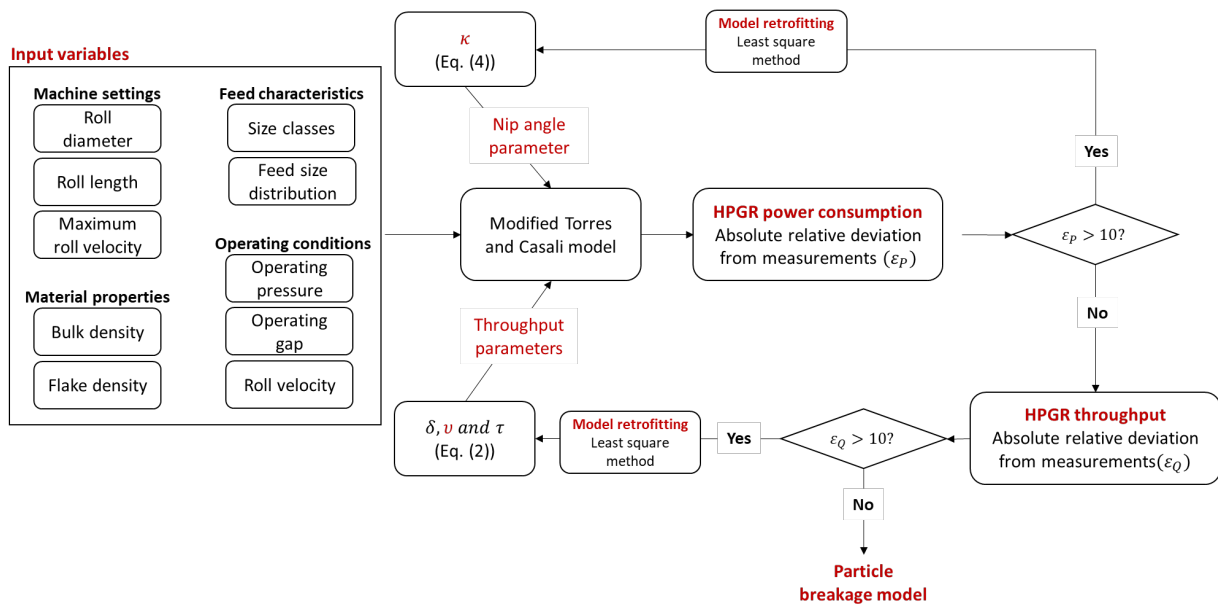


FIG 8 – Approach used to recalibrate model parameters based on the deviations in model prediction owing to roll wear. ϵ_Q and ϵ_P are the absolute relative deviation from measurements for the throughput and power consumption, respectively.

Figure 9 then presents the comparison between model and experiments when the approach presented in Figure 8 was applied. Results showed very good agreement over the entire period, with absolute relative deviations of simulations to measurements up to 4.8 per cent for power consumption and 6.0 per cent for throughput. The approach adopted seems to be able to circumvent the bias in the model prediction when dealing with worn rolls, as well as minor variations in feed competence. Nevertheless, results from Figure 9b shows the model limited the ranges of predicted values for HPGR throughput from October to December 2017. These poor predictions may be explained, at least in part, by the simplified assumption of recalibrating some model parameters to compensate the error of the operating gap measurement, which may be regarded as a disadvantage of the algorithm.

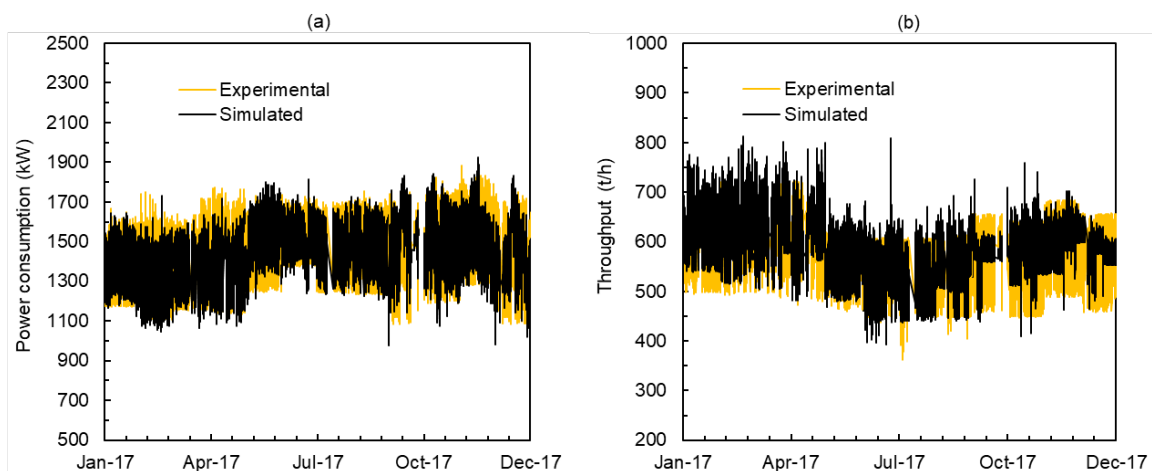


FIG 9 – Comparison between experimental and predicted power consumption (a) and throughput (b) in a period of twelve months assessed after applying the calibration approach depicted in Figure 8. Data is presented for every 5 min of operation.

Size reduction model

Feed size distribution prediction

To ensure a reliable assessment of the size reduction in the entire period, data from laboratory analyses were reconciled with supervisory system data. Reconciliation assumed that the measurement made of the BSA would be a process average over the last four hours, so that this value was repeated for the four hours prior to the measurement. Additionally, taking into account the key model requirement of using the complete feed size distribution as an input, the present work proposes that the feed sizes follows a Rosin-Rammler distribution function, given by:

$$P_i = 1 - \exp \left[- \left(\frac{x_i}{x^*} \right)^\alpha \right] \quad (14)$$

where x_i is particle size (mm) and x^* is a 62.3 per cent passing size (mm). Based on an extended database containing 162 measurements of BSA and size distributions presented elsewhere (Campos *et al*, 2021), a relationship was then proposed to calculate the size parameter x^* as a function of the Blaine specific surface area. Figure 10 presents the relationship between these two variables for 80 per cent of the database, which was randomly selected as calibration data set. The clear linear relationship between this parameter and BSA suggests that simple linear equation to describe it, represented by:

$$x^* = 126.5 - 0.0412BSA_{Alim} \quad (15)$$

where x^* is given in μm and BSA_{Alim} is the Blaine specific surface area (cm^2/g) from the HPGR feed gathered from laboratory measurements. The parameter α in Equation 14 was set to the optimal constant value of 0.97. Predictions made using Equation 14 were then compared to the respective experimental size distributions for both calibration data sets (80 per cent used for training) and validation data set (the remaining 20 per cent of the original data set) using Equation 13. Results demonstrate the good predictive capabilities of the model with average values for the objective function for calibration and validation data sets of 0.04 and 0.06, respectively. Figure 10 still presents the region bounds by the dotted red lines with relative deviations between model (black line) and fitted sizes (green circles) up to 10 per cent.

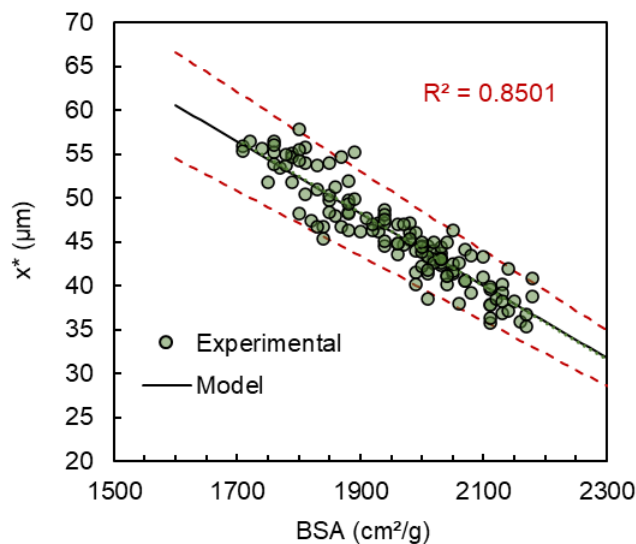


FIG 10 – Relationship between BSA for several measurements carried out elsewhere (Campos *et al*, 2021) and the critical size fitted in Equation 14. Green circles are values fitted from Equation 14 and the black line is the model fitting with Equation 15. The red dotted lines bound the region with relative deviations between black line and experiments up to 10 per cent.

Product BSA

In order to simulate the size reduction in the HPGR the breakage model was calibrated based on survey data. All five parameters from the breakage function (Equation 7) and two parameters from the selection function (Equation 9) were assumed to remain constant and equal to previous

calibration carried out by the authors (Campos *et al*, 2019b). The remaining parameter from the selection function (s_1^E) was then fitted on the basis of a reference test selected among the ones when the HPGR was operating under good wear conditions and in the beginning of roll life.

As such, considering the model presented in Equations 14 and 15 and the breakage parameter depicted above, Figure 11 presents the comparison between experimental and predicted values for the HPGR product BSA when considering a constant and average feed size distribution with 1550 cm²/g in a period of 740 hours of operation. This simplified assumption was adopted in order to check the real effect of the feed size distribution in the model prediction. Indeed, as discussed in Figure 6, there is a clear trend between both HGPR feed and product, being the second one strongly determined by the first. Analysing both results together allows to explain the poor agreement between model and experiments presented in Figure 11.

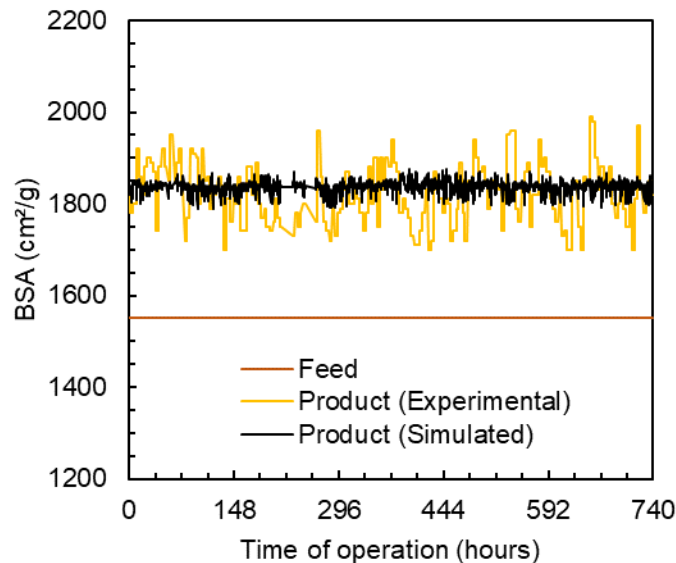


FIG 11 – Comparison between experimental and predicted value for the HPGR product BSA considering a fixed feed size distribution with 1550 cm²/g.

Figure 12 then presents a more complete version of the model dealing with the measured feed size distribution in real time. First it is worth highlighting the variation of the HPGR product over the entire period assessed following the trend imposed by the HPGR feed. Nevertheless, results from Figure 12 show the very good agreement between experimental and predicted values for the HPGR product BSA with average absolute relative deviation from measurements equal to 2.7 per cent. Results also allow to conclude that the model is able to capture key variations in the feed size distribution and accurately describe the HPGR product. Results for the twelve months assessed also presented good agreement with average absolute relative deviation from measurements of up to 5.3 per cent, but results were omitted for brevity. The predicted HPGR product BSA was calculated on the basis of the predicted product size distribution using a method proposed and calibrated previously by the authors (Campos *et al*, 2021).

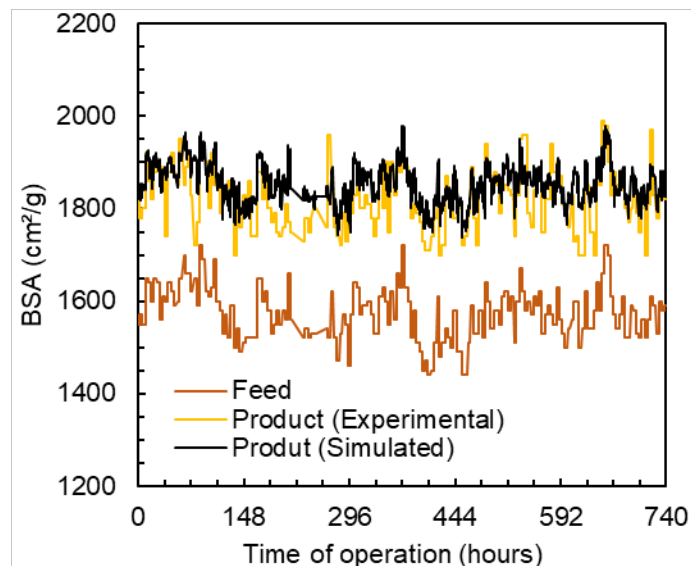


FIG 12 – Comparison of experimental and predicted values for the HPGR product BSA on the basis of the feed BSA measured every 4 hours.

CONCLUSIONS

The work relied on the application of the Modified Torres and Casali model as pseudo-dynamic approach to describe an industrial-scale HPGR pressing iron ore concentrates. Good agreement was reached to predict power consumption, throughput and product BSA when the HPGR was operating under good roll wear conditions.

Evidence of a bathtub wear profile and a wear parabolic profile after a period of 14 000 hours of operation was presented as a great challenge for model descriptions. Results highlighted an underestimation of power and throughput when the HPGR started operating under significant roll wear patterns. An algorithm was proposed to optimise selected model parameters with the aim of improving prediction for the HPGR with worn rolls which provided very good agreement between model and experiments.

A model was also proposed to convert the HPGR feed BSA into a cumulative feed size distribution. The model was validated under a wide range of measurements. Application of the breakage model using this new feature provided very good agreement between product BSA measured and predicted by the model.

Results showed feasibility of applying the model as a pseudo-dynamic model and coupled with real-time information to describe the HPGR performance in an industrial-scale plant pressing iron ore concentrates.

ACKNOWLEDGEMENTS

We thank you Vale S.A for the financial and technical support and the Brazilian agency CNPq for the additional financial support.

REFERENCES

- Abazarpoor, A, Halali, M, Hejazi, R and Saghaeian, M, 2018. HPGR effect on the particle size and shape of iron ore pellet feed using response surface methodology. *Mineral Processing and Extractive Metallurgy*, 127(1), 40–48.
- Barrios, G K P and Tavares, L M, 2016. A preliminary model of high pressure roll grinding using the discrete element method and multi-body dynamics coupling, *Int. J. Miner. Process.* 156, 32–42.
- Burchardt, E and Mackert, T, 2019. HPGRs in minerals: what do more than 50 hard rock hpgrs tell us for the future? (Part 2–2019). *Proceeding of SAG Conference*, (2), 15–36.
- Campos, T M, Bueno, G and Tavares, L M, 2021. Modeling comminution of iron ore concentrates in industrial-scale HPGR. *Powder Technology*, 383, 244–255.
- Campos, T M, Bueno, G, Barrios, G K and Tavares, L M, 2019a. Pressing iron ore concentrate in a pilot-scale HPGR. Part 1: Experimental results. *Minerals Engineering*, 140, 105875.

- Campos, T M, Bueno, G, Barrios, G K and Tavares, L M, 2019b. Pressing iron ore concentrate in a pilot-scale HPGR. Part 2: Modeling and simulation. *Minerals Engineering*, 140, 105876.
- Chelgani, S C, Nasiri, H and Tohry, A, 2021. Modeling of particle sizes for industrial HPGR products by a unique explainable AI tool-A 'Conscious Lab' development. *Advanced Powder Technology*, 32(11), 4141–4148.
- Cleary, P W and Sinnott, M D, 2021. Axial pressure distribution, flow behaviour and breakage within a HPGR investigation using DEM. *Minerals Engineering*, 163, 106769.
- Daniel, M J, 2002. HPGR Model Verification and Scale-up, Masters Thesis. Julius Kruttschnitt Mineral Research Centre, University of Queensland, Brisbane.
- Dundar, H, Benzer, H and Aydogan, N, 2013. Application of population balance model to HPGR crushing. *Minerals Engineering*, 50, 114–120.
- Gardula, A, Das, D, DiTrento, M and Joubert, S, 2015. First year of operation of HPGR at Tropicana Gold Mine—Case Study. *Cuprum: czasopismo naukowo-techniczne górnictwa rud*, (2), 15–36.
- Herbst, J A and Fuerstenau, D W, 1980. Scale-up procedure for continuous grinding mill design using population balance models. *International Journal of Mineral Processing*, 7(1), 1–31.
- Johansson, M and Evertsson, M, 2019. A time dynamic model of a high-pressure grinding rolls crusher. *Minerals Engineering*, 132, 27–38.
- King, R P, 2001. *Modeling and simulation of mineral processing systems*. Elsevier.
- Morrell, S, Lim, W, Shi, F and Tondo, L, 1997. Modelling of the HPGR Crusher. *Comminution Practices*, 117–126.
- Nejad, R K and Sam, A, 2017. Limitation of HPGR application. *Mineral Processing and Extractive Metallurgy*, 126(4), 224–230.
- Numbi, B P and Xia, X, 2015. Systems optimization model for energy management of a parallel HPGR crushing process. *Applied Energy*, 149, 133–147.
- Rashidi, S, Rajamani, R K and Fuerstenau, D W, 2017. A review of the modeling of high pressure grinding rolls. *KONA Powder and Particle Journal*.
- Rodriguez, V A, Barrios, G K, Bueno, G and Tavares, L M, 2021. Investigation of Lateral Confinement, Roller Aspect Ratio and Wear Condition on HPGR Performance Using DEM-MBD-PRM Simulations. *Minerals*, 11(8), 801.
- Rodriguez, V A, Barrios, G K, Bueno, G and Tavares, L M, 2022. Coupled DEM-MBD-PRM simulations of high-pressure grinding rolls. Part 1: Calibration and validation in pilot-scale. *Minerals Engineering*, 177, 107389.
- Torres, M and Casali, A, 2009. A novel approach for the modelling of high-pressure grinding rolls. *Minerals Engineering*, 22(13), 1137–1146.
- Van der Meer, F P, 1997. Roller Press Grinding of Pellet Feed. Experiences of KHD in the Iron Ore Industry. *AusIMM Conference on Iron Ore Resources and Reserves Estimation*, n. September, pp. 1–15.
- Van Der Meer, F P, 2010. HPGR Scale-Up and Experiences. In *XXV International Mineral Processing Congress*, pp. 6–10.
- Vyhmeister, E, Reyes-Bozo, L, Rodriguez-Maecker, R, Fúnez-Guerra, C, Cepeda-Vaca, F and Valdés-González, H, 2019. Modeling and energy-based model predictive control of high pressure grinding roll. *Minerals Engineering*, 134, 7–15.